

Dynamics of Apparent and Event Horizons

Peter Anninos,¹ David Bernstein,^{1,*} Steven Brandt,^{1,3} Joseph Libson,^{1,3} Joan Massó,^{1,2} Edward Seidel,^{1,3}
Larry Smarr,^{1,3} Wai-Mo Suen,⁴ and Paul Walker^{1,3}

¹National Center for Supercomputing Applications, Beckman Institute, 405 North Mathews Avenue, Urbana, Illinois 61801

²Departament de Física, Universitat de les Illes Balears, E-07071 Palma de Mallorca, Spain

³Department of Physics, University of Illinois, Urbana, Illinois 61801

⁴McDonnell Center for the Space Sciences, Department of Physics, Washington University, St. Louis, Missouri 63130

(Received 28 February 1994)

We have developed a powerful and efficient new method in numerical relativity for locating the event horizon to high accuracy, making possible the study of horizon dynamics in highly nonlinear black-hole spacetimes. We analyzed and compared evolutions of the apparent and event horizons of both Schwarzschild and Kerr black holes struck by strong bursts of gravitational radiation, and of colliding black holes. In all black-hole spacetimes studied, the horizons oscillate with the quasinormal frequency at late times.

PACS numbers: 04.70.Bw, 04.20.Dw, 04.25.Dm, 04.30.Db

Black holes are among the most fascinating predictions in the theory of general relativity. The essential characteristics of a black hole in relativity are its horizons, in particular the apparent horizon (AH) and the event horizon (EH). The AH is defined as the outermost trapped surface of a region in space, whereas the EH is defined as the boundary of the causal past of the future null infinity [1]. In this paper, we study and compare the dynamics of the AH and EH for various spacetimes.

The AH is defined locally in time and hence is much easier to locate than the EH in numerical relativity (see, e.g., Ref. [2]). Here we discuss a method to find the EH, given a numerically constructed black-hole spacetime going through violent processes and settling down to a stationary state at late times. (If the numerical evolution is stopped during the violent phase, the question of locating the horizon is meaningless.) In principle the EH can be found by tracing the path of null rays through time. Outward going light rays emitted just outside the EH will diverge away from it, escaping to infinity, and those emitted just inside the EH will fall away from it, towards the singularity. In a numerical integration it is difficult to follow accurately the evolution of a horizon generator forward in time, as small numerical errors cause the ray to drift and diverge rapidly from the true EH. It is a physically unstable process. But we can actually use this property to our advantage by considering the time-reversed problem. In a global sense in time, any outward going photon that begins near the EH will be *attracted* to the horizon if integrated *backward* in time [3]. In integrating backwards in time, we shall show that it suffices to start the photons within a region where the EH is expected to reside. Such a region is often easy to determine after the spacetime has settled down to stationarity. For example, the photons can be started near the AH if it is known at late times, although such a choice is not necessary. Our first generation horizon finder was

based on this “backward photon” method, which worked well for all numerically constructed spacetimes that we tested it on.

Building on the backward photon method, we developed a second generation horizon finder based on a “backward surface” method, which evolves the entire null surface instead of individual photons. A generator of a null surface is guaranteed to satisfy the geodesic equation [4]. A null surface defined by $f(t, x^i) = 0$ satisfies the condition

$$g^{\mu\nu} \partial_\mu f \partial_\nu f = 0. \quad (1)$$

Hence the evolution of the surface can be obtained by a simple integration,

$$\partial_t f = \frac{-g^{ti} \partial_i f + \sqrt{(g^{ti} \partial_i f)^2 - g^{tt} g^{ij} \partial_i f \partial_j f}}{g^{tt}}. \quad (2)$$

The advantages to integrating an entire surface include the following: (i) Equation (2) is first order, unlike the geodesic equation used in integrating photons which is second order and requires the initial directions of the photons to be specified. In integrating the geodesic equation, the photons are attracted along the normal direction to the EH, but there is no such attractive property in the tangential direction. Hence the trajectories of the photons are sensitive to the initial choice in the tangential direction, and may further drift tangentially due to inaccuracies in the integration. This drifting may cause neighboring generators to cross, complicating the identification of true horizon caustics. Such tangential drifts impose high accuracy requirements to make an initial surface of photons remain surface forming after integration. In the surface method, tangential drifting and the question of the initial tangential direction do not exist because the only direction that a surface can move is normal to itself. (ii) Equation (2) contains

only derivatives of the surface and *not* of the metric components themselves and is therefore less susceptible to the numerical inaccuracies present in the metric data, as compared to the integration of the geodesic equation.

Using this backward surface method we are able to trace accurately and efficiently the entire history of the EH in numerically constructed spacetimes. For an axisymmetric spacetime representing a black hole interacting with a gravitational wave (the first case detailed below) resolved on a grid of 200 radial by 53 angular zones and evolved to $t = 75M$ (where M is the mass of the black hole), it takes just a few minutes for the backward surface method to trace the EH on a computer workstation, and about twice as long for the backward photon method. We contrast our "backward" methods with another method [5] that uses forward integration of individual photons to find the EH.

The first case we discuss consists of a nonrotating black hole surrounded by an axisymmetric gravitational wave initially at a finite distance away from the hole. The system was evolved with a code described in Refs. [6,7]. The black hole becomes distorted as the incoming wave hits. In time, it settles down and returns to a Schwarzschild hole with a larger mass. Figure 1 shows the areas of eight different integrations of the EH starting at different places. In one case the AH was used as an initial surface for the integration. Because the AH is *inside* the correct location of the EH, the surface expands outward as it is attracted to the correct location. In other cases, surfaces larger or smaller than the AH are chosen as initial guesses. Note that in all cases the surfaces are attracted to the

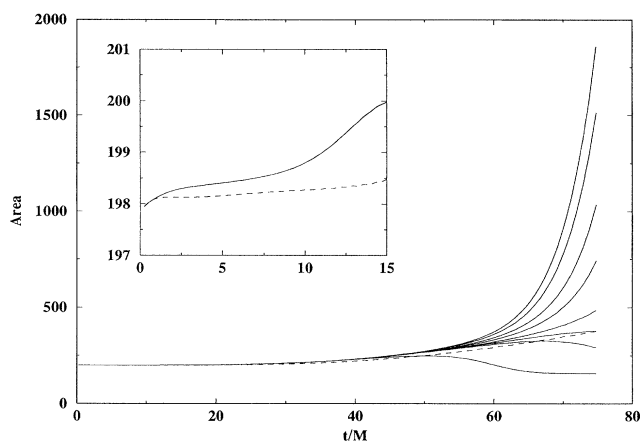


FIG. 1. The area of the event horizon is traced through time for different initial surfaces (solid lines), and compared to the area of the apparent horizon (dashed line). The attracting nature of the event horizon is dramatic, as all of our backward surface integrations trace the same path, although they start from very different initial locations. The inset shows an expanded view of the early time results. *All* surface integrations are shown, and are completely indistinguishable. The initial increases in the surface areas in the inset near $t = 0$ are caused by a small amount of energy near the horizon in the initial data.

same surface in precise detail, as they should be. As the test surfaces coincide to much less than $\frac{1}{10}$ th of the grid separation (corresponding to typical proper distances between the surfaces of less than $0.01M$) for the range $t = 0$ to $40M$, we have located the event horizon to such an accuracy in this range. We have checked that all photons fired just inside this surface will fall into the singularity, while photons fired just outside can escape to infinity. The inset shows an expanded view of the early time. All surfaces computed are shown, but they are completely indistinguishable in spite of their extremely different starting positions, clearly showing the power and stability of this method. At $t = 0$ the AH and EH practically coincide with each other. Then the EH foresees the coming of the wave and expands. As the wave is falling in, after about $t = 15M$, the AH starts to expand and catch up. The behavior of the AH and EH are exactly as expected. To demonstrate that the shapes of the surfaces are the same, we show in Fig. 2 the coordinate locations of several of these surfaces at various times. At the beginning of integration ($t = 72.5M$), the surfaces are very different. For smaller t values, they become practically identical.

The ability to determine accurately the AH and EH for dynamical holes opens up the possibility for the first time of using the horizons as a tool to study black-hole physics in numerical relativity. As a first example of this, we show in Fig. 3 a geometric embedding of the coalescing horizons for the head-on collision of two black holes, as discussed in Refs. [8,9]. The embedding, which preserves the proper surface areas of the horizons, shows not just the

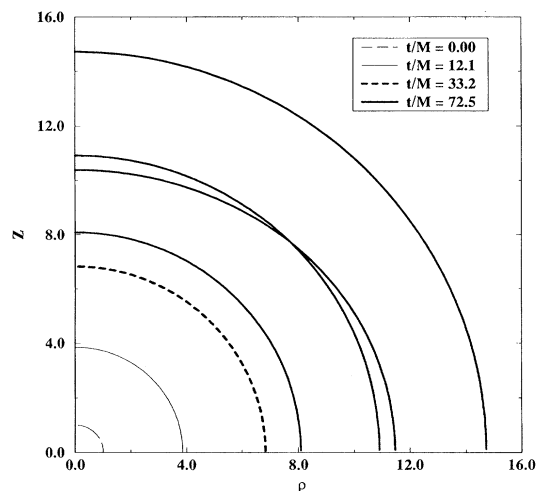


FIG. 2. The coordinate locations of the innermost, outermost, and two other test surfaces used in Fig. 1 are shown for various times. The initial trial surfaces are very different at the start of the backward integration ($t/M = 72.5$). However, they quickly converge to the same surface, and are indistinguishable at earlier time. Although the coordinate position of the surfaces looks quite spherical, their intrinsic geometry is much less spherical.

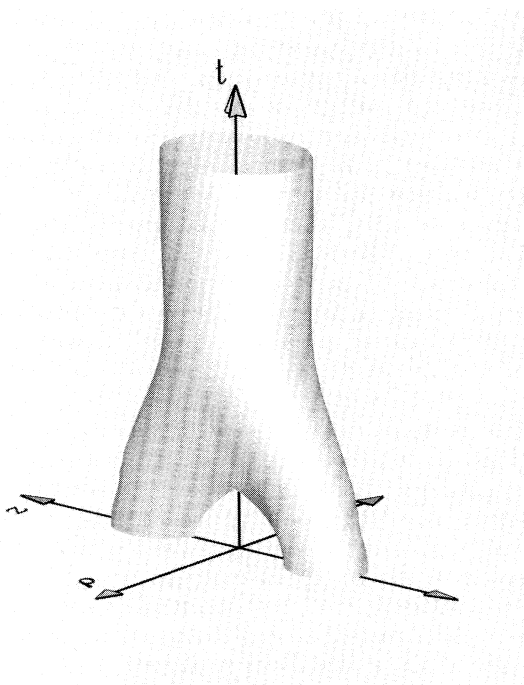


FIG. 3. The geometric embedding of the event horizon for two black holes colliding head on is shown. The z coordinate marks the symmetry axis, and t is the coordinate time (shown only up to $t = 25M$). Initially the two holes are separated but eventually coalesce into a single black hole.

topology but also the geometric properties of the horizon. Although such a picture of the embedding is familiar, this is the first time it has actually been computed. There have been a number of attempts to estimate the critical distance beyond which these initial data sets contain two separate black holes [10], and with our method we can now say that there are two holes for the separation parameter μ greater than about 1.8 (corresponding to a proper distance between horizons of about $L = 7M$, where M is the mass of each hole). The horizon shown in Fig. 3 corresponds to $\mu = 2.2$ ($L = 8.92M$). We have also checked that the surface shown gives the correct location of the event horizon to less than one-tenth of the grid separation based on both the convergence of null surfaces and the photon tests before and after the coalescence. Note that before the coalescence there is a line of caustics on the “inner seam of the trouser legs.” Along this caustic line, the horizon surface has a cusp, at which point only one-sided normal vectors are defined. In this paper we use one-sided derivatives to evaluate the right hand side of Eq. (2) at those points. Alternatively the entire null surface can be evolved, including the portion that leaves the horizon, so the entire surface remains smooth and no special treatment is needed anywhere [11]. We note that this line of caustics is spacelike, which has been verified numerically.

In Fig. 4 we show the embedding of the equator of the EH for an axisymmetrically distorted Kerr black hole evolved with a code described in Ref. [12]. We also show the generators themselves, computed from the gradient of the surface (see [13] for more details of this procedure). The rotation of the hole causes the generators to be dragged along, forming the famous “barber pole twist,” another familiar picture now calculated for the first time. We see that the “pole” is distorted by the incoming gravitational wave.

We can also use the AH and EH together to study black-hole dynamics. In Fig. 5(a) we show the ratio of the polar to equatorial circumference C_p/C_e of both the AH and EH for the first case discussed above. (Note that the horizon begins and ends as a sphere with a Gaussian curvature that is constant to within 1 part in 10^6 , which shows clearly that the hole was “Schwarzschild” at both times. This also provides a stringent test for our event horizon finder, since it must trace a surface backward in time as it undergoes a period of distortion, and then return to a sphere.) We see that the AH and EH oscillate in precisely the same manner, despite the fact that one is a null surface while the other is spacelike. These oscillations of the horizons are caused by the “quasinormal modes” (QNM) of the black-hole spacetime. As the waves leak out to infinity and down the hole, those going down cause the horizons to oscillate. In the membrane point of view [14], the oscillations are dissipated into viscous heating of the horizon membrane, causing the horizon surface area to increase during the

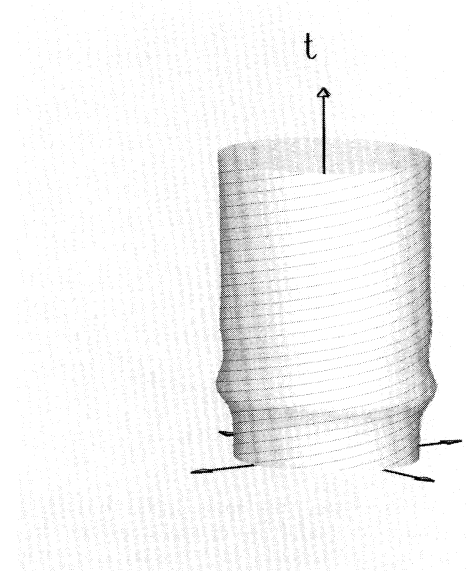


FIG. 4. The embedding of the event horizon, with generators, is shown for a rotating black hole distorted by incoming gravitational radiation. The evolution of the equator up to $t = 75M$ is shown with the polar direction suppressed. Note the barber pole twist of the generators caused by the rotation of the hole.

oscillations as we have seen in our calculations. We show a fit of the EH oscillation to the two lowest $\ell = 2$ QNM's of the black hole as determined in linear perturbation theory (the initial incoming Brill wave is predominantly in the $\ell = 2$ mode). The fit is remarkable, showing conclusively that both the AH and EH oscillate at the QNM of the black hole. (The horizons oscillate at the QNM frequency in coordinate time, as the spacetime is basically stationary for the region outside the horizon. Although the lapse is less than one near the horizon, it is basically time independent, so the frequency of waves measured in coordinate time is the same as that measured at infinity.) In Fig. 5(b) we show a similar graph for the two black-hole collision case of Fig. 3, establishing the generic nature of these results. The same kind of oscillations is also clear in the horizon embedding diagram Fig. 4, although here the polar direction is suppressed.

Our method can find event horizons without knowledge of the apparent horizon, so it should be a useful tool for analyzing spacetimes even in cases where the apparent horizon cannot be found (e.g., if the time slicing does not intersect the apparent horizon). Its impact on the numerical investigations of the cosmic censorship conjecture and the hoop conjecture (vacuum version [15]) could prove interesting.

We are most grateful to Kip Thorne for contributing ideas and suggesting improvements and additions to this

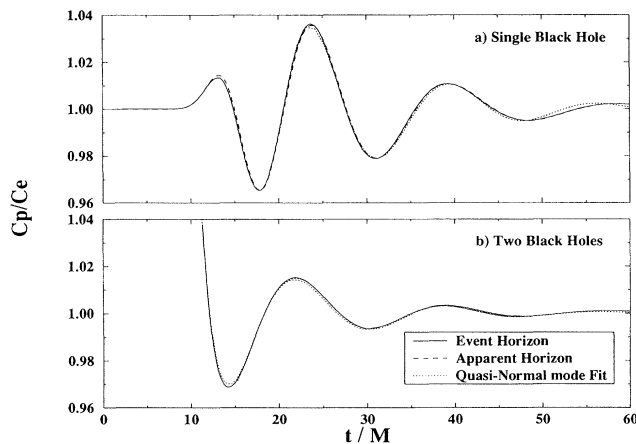


FIG. 5. The ratio C_p/C_e of the polar circumference to the equatorial circumference of both the event horizon (solid line) and apparent horizon (dashed line) is shown versus coordinate time t for both the distorted Schwarzschild hole case of Fig. 1 (a) and the two black-hole collision (b) after the coalescence. The dot-dashed line shows the fit of the two lowest $\ell = 2$ quasinormal modes to the event horizon. Both the AH and EH oscillate at the quasinormal frequency.

revised manuscript. We thank Richard Isaacson and Richard Matzner for useful discussions. We also thank Scott Hughes, Charles R. Keeton, II, Stuart Shapiro, Saul Teukolsky, and Kevin Walsh for allowing us to use the Cornell code for making comparisons with our code, and especially S.H., C.R.K., and K.W. who, together with one of us (P.W.), developed some of the I/O routines used in the present version of our code. J.M. acknowledges a fellowship (P.F.P.I.) from Ministerio de Educación y Ciencia of Spain. This research is supported by the NCSA, the Pittsburgh Supercomputing Center, and NSF Grants No. PHY91-16682, No. PHY94-04788, No. PHY94-07882, and No. ASC93-18152.

*Present address: Department of Mathematics, Statistics and Computing Science, University of New England, Armidale, NSW 2351, Australia.

- [1] S. W. Hawking and G. F. R. Ellis, *The Large Scale Structure of Spacetime* (Cambridge University Press, Cambridge, 1973).
- [2] G. Cook and J. York, *Phys. Rev. D* **41**, 1077 (1990).
- [3] Strictly speaking this is true only in a global sense, but not at each instant of time. A detailed discussion of this will be given elsewhere.
- [4] B. Carter, in *General Relativity: An Einstein Centenary Survey*, edited by S. Hawking and W. Israel (Cambridge University Press, Cambridge, 1979).
- [5] S. Hughes, C. R. Keeton, II, P. Walker, K. Walsh, S. L. Shapiro, and S. A. Teukolsky, *Phys. Rev. D* **49**, 4004 (1994).
- [6] D. Bernstein, D. Hobill, E. Seidel, J. Towns, and L. Smarr, *Phys. Rev. D* **50**, 5000 (1994).
- [7] P. Anninos, D. Hobill, E. Seidel, L. Smarr, and J. Towns, *Numerical Astrophysics* (Springer-Verlag, New York, 1994).
- [8] P. Anninos, D. Hobill, E. Seidel, L. Smarr, and W.-M. Suen, *Phys. Rev. Lett.* **71**, 2851 (1993).
- [9] P. Anninos, D. Hobill, E. Seidel, L. Smarr, and W.-M. Suen (to be published).
- [10] L. Smarr, in *Sources of Gravitational Radiation*, edited by L. Smarr (Cambridge University Press, Cambridge, 1979), p. 245.
- [11] We thank Kip Thorne for this suggestion.
- [12] S. Brandt and E. Seidel, Proceedings of the Penn State Numerical Relativity Meeting, 1993; also (to be published).
- [13] J. Libson, J. Massó, E. Seidel, W.-M. Suen, and P. Walker (to be published).
- [14] *Black Holes: The Membrane Paradigm*, edited by K. S. Thorne, R. H. Price, and D. A. Macdonald (Yale University Press, London, 1986).
- [15] E. Flanagan, *Phys. Rev. D* **44**, 2409 (1991).

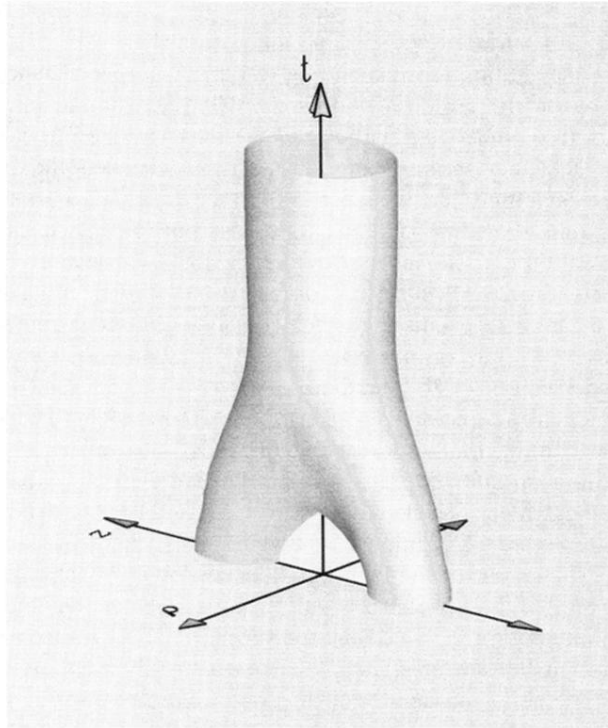


FIG. 3. The geometric embedding of the event horizon for two black holes colliding head on is shown. The z coordinate marks the symmetry axis, and t is the coordinate time (shown only up to $t = 25M$). Initially the two holes are separated but eventually coalesce into a single black hole.

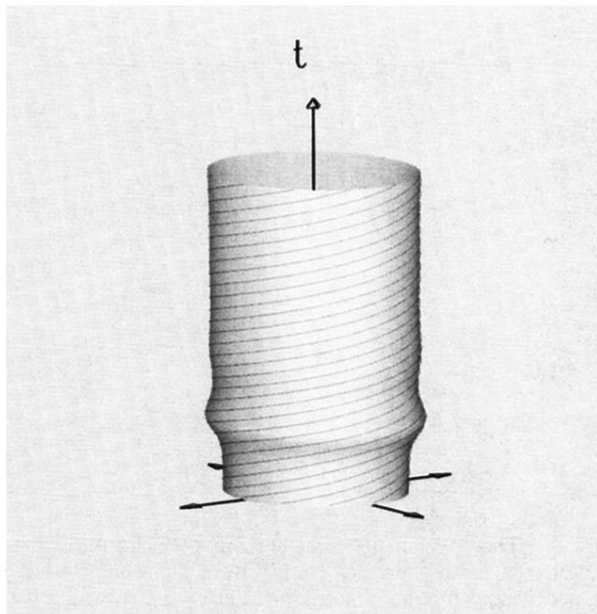


FIG. 4. The embedding of the event horizon, with generators, is shown for a rotating black hole distorted by incoming gravitational radiation. The evolution of the equator up to $t = 75M$ is shown with the polar direction suppressed. Note the barber pole twist of the generators caused by the rotation of the hole.